PNC-TN9410 88-044

Erosion-Corrosion Experiments and the Quantitative Equations under Water-Vapour Two-Phase Flows

May , 1988

OARAI ENGINEERING CENTER
POWER REACTOR AND NUCLEAR FUEL DEVELOPMENT CORPORATION

複製又はこの資料の入手については，下記にお問い合わせください。
〒311-13　茨城県東茨城郡大洗町成田町4002
動力炉・核燃料開発事業団
大洗工学センター　システム開発推進部・技術管理室

Enquires about copyright and reproduction should be addressed to: Technology Management Section O-arai Engineering Center, Power Reactor and Nuclear Fuel Development Corporation 4002 Narita-cho, O-arai-machi, Higashi-Ibaraki, Ibaraki-ken, 311-13, Japan

動力炉・核燃料開発事業団（Power Reactor and Nuclear Fuel Development Corporation）

EROSION-CORROSION EXPERIMENTS AND THE QUANTITATIVE EQUATIONS UNDER WATER-VAPOUR TWO-PHASE FLOWS*

Mitsutaka Koike** and Hiroshi Baba**

O-arai Engineering Center
Power Reactor & Nuclear Fuel Development Corporation (PNC)
4002 O-arai-machi, Ibaraki-ken 311-13, Japan,
Tel. 0292-67-4141

Abstract

Erosion experiments of stainless steel were performed under water-vapour two-phase flow conditions. The experiments were performed by using Component Test Loop and erosion losses were estimated by weight differences of specimens between before and after tests.
Quantitative erosion-corrosion equations both under two-phase flows and under single-phase flows were proposed by semi-theoretical considerations with the present results. Also, the quantitative erosion/corrosion equation was originally made for all metals.

---

* Presented at the 1988 JAIF International Conference on Water Chemistry in Nuclear Plants, Operational Experience and New Technologies for Management, Tokyo, Japan, April 19-22, 1988

** Systems and Component Development Section (機器システム開発室)
小池 通崇, 馬場 博

1. Introduction

Power Reactor and Nuclear Fuel Development Corporation (PNC) in Japan has developed the ATR-Fugen, a 165MWe prototype boiling-light-water-cooled heavy-water-moderated pressure tube-type reactor of Japan, which has operated satisfactorily since the start of commercial operation in March 1979. It achieved the total electrical generation of 8.1×10^9KW·h in January 1988. A 600MWe ATR Demonstration Plant has been designed on the basis of the experience of the Fugen and is scheduled to begin commercial operation at the end of 1990's. The ATR is a unique reactor designed mainly to use plutonium -uranium mixed oxide (Mox) fuels (1).

The demonstration reactor has 648 outlet pipes in which high-speed two-phase water (ca.280°C, 70kg/cm^2) flows upwards from pressure tube to steam drum. The outlet pipes are made of type 316L stainless steel of nuclear grade and about 3 inches in size.

The design value of average steam phase velocity of two-phase flow in the outlet pipes for the Demonstration Reactor is about 14m/sec, and that of the maximum steam velocity is about 20m/sec. Design values of the average and maximum steam qualities in the outlet pipes are about 16% and 30%, respectively. It must be certified that outlet pipes are endurable under these conditions throughout the life of the reactor operation. There have been few erosion experiments of water-vapour two-phase flow for steam qualities of 10~30 %. Therefore, erosion experiments of type 316L stainless steel

were conducted in this work under water-vapour high-speed two-phase flow conditions, with parameters of steam quality and flow speed by the use of Component Test Loop (CTL) at O-arai Engineering Center of PNC. The CTL is a full-scale test facility simulating the primary cooling circuit of the ATR in terms of coolant temperature and pressure.

In respect of the erosion under water-vapour two-phase flows, there are few erosion experiments and also few erosion theories. This paper describes erosion experiments performed and a theory proposed under water-vapour two-phase flow conditions. Also, we have made quantitative erosion-corrosion equations both under two-phase flows and under single-phase flows. Besides, we have originally made the quantitative erosion/corrosion equation for all metals by semi-theoretical considerations.

2. Experimental Procedure

Erosion experiments were performed by the use of the CTL in which high-temperature pressurized two-phase water-vapour is circulated. Figure 1 shows the schematic flow diagram of the CTL. A Boiler supplies heat to water and Circulation Pumps supply head to water in the CTL. Water-vapour two-phase flow is produced by mixing hot water and steam. After they are mixed, the two-phase water-vapour flows into erosion test sections and to a Direct Condenser which separates varpour from two-phase flow. Vapour is circulated by a Steam Compressor with high speed.

Four kinds of erosion test sections are made in order to achieve four kinds of flow speed tests by varying the pipe diameter of each test section. Many small pipe specimens cut in round slices are lines in series and fixed in four erosion test sections of the CTL. These inner diameters are 73.7, 62.1, 49.4 and 38.3mm. The erosion test apparatus is shown in Figure 2 in which test specimens, fixing liner etc. are represented. Specimens are inserted into liners and the liners lined in series are also inserted into the pipe and fixed. In Figure 2 are shown straight specimen, bend specimen, inner bend specimen and outer bend specimen. Specimen's weight is measured before and after the erosion test. The two-phase flow rate is constant during experiment, so that the velocity of the flow is increased as the diameter of the test section becomes smaller. The erosion experiment with four kinds of velocities is to be performed by a constant

flow rate test. In order to estimate the erosion loss for the outlet pipes under two-phase water-vapour flow conditions, not plate type specimens but pipe type specimens must be used for the experiments, because the two-phase flow pattern is very complicated compared with single phase flow pattern and plate type specimens are not appropriate to the erosion test for the outlet pipes. The two-phase flow pattern of the present experiments are classified into annular mist flow type [2].

Table 1 shows the chemical composition of the material used for specimens of the present work. Erosion experiments were carried out under various conditions with parameters of water chemistries, steam qualities, experimental periods and flow velocities. Under water-vapour two-phase flow conditions, two kinds of experiments designated as AVT (I ~ IV) and NT (I ~ III) were performed, where AVT and NT represent all volatile treatment and neutral treatment of the water, respectively. Under single-phase flow conditions, heated water and steam experiments designated as AVT (V) and AVT (VI) respectively were performed. Experimental conditions were all listed in Table 2.

The erosion loss of material was estimated from the specimen weight difference between before and after erosion tests. The erosion loss ΔW is expressed as

$$\Delta W = W_1 - W_0 \qquad ,(1)$$

where W_0 is an initial specimen weight before test, and W_1 is a specimen weight when after the test oxide film on the specimen is removed by chemical reagents. Chemical reagents used here removed oxide film only and did not attack base metal, which were examined by the blank test.

The flow speeds of the water-vapour two-phase flow were calculated by the use of quality x and void fraction α. Void fractions are obtained by the equations of Bankoff and Jones [3].

Erosion specimens after tests were observed on the inner surfaces by the use of Scanning Electron Microscope (SEM) to detect whether severe erosions were ocurred or not. Analyses using Auger Electron Spectroscopy (AES) were performed on oxide films of specimen surfaces, especially for oxygen element. By etching oxide films up to base metal with the use of argon ions, fractions of elements which compose films were obtained quantitatively. Also, X-ray diffraction analyses were performed on the films to determine chemical formulae of the oxides.

3. Experimental Results

Test items are listed in Table 2 and experimental results are listed in Table 3. In Table 3, all of the data are summarized, in which the erosion loss of type 316L stainless steel are represented in the unit of reduced thickness per year, μm/year.

3.1 AVT Erosion Results under Two-Phase Flow

AVT erosion experiments under two-phase flow consist of AVT(I) (x=15%, straight and bend specimens), AVT(Ⅱ) (x=15%, bend specimens), AVT (Ⅲ) (x=26%, straight and bend specimens) and AVT (IV) (x=60%, straight and bend specimens) ones.

Experimental results of AVT(I) (straight specimens), AVT(Ⅲ) (straight specimens) were already published [4]. Here, Figure 3 shows the experimental data for AVT(Ⅱ) test of bend specimens which consist of inner bend specimen and outer bend specimen. The steam quality of 15% is about the average value of the design value. Test temperature and pressure are like those of the design values, and the water chemistry is determined by the all volatile treatment in which dissolved oxygen (DO) is very low (less than 2ppb). White circle represents inner bend specimen data and black triangle represents outer bend specimen data. Abscissa represents the steam phase velocity and ordinate represents the erosion loss of type 3161 stainless steel. The period of the test was about 1000 hours. Erosion losses were very samll in general and erosion losses of steam phase velocity

of about 40 m/s were slightly larger than those of any other velocities.

Figure 4 shows the experimental data for AVT (IV) test (x=60%) of straight specimens and bend specimens. The period of the test is 544 hours. White circle represents straight specimen data and white triangle represents bend specimen data. Erosion losses were very small in general and erosion losses of straight specimens were rather larger than those of bend specimens.

3.2 NT Erosion Results under Two-Phase Flow

NT erosion experiments under two-phase flow consist of NT(I) (x=15%, straight specimens), NT(II) (x=15%, straight specimens) and NT (III) (x=15%, bend specimens) ones.

Experimental results of NT(I) (170 hours) were already published [4]. Here, FIgure 5 shows the experimental data for NT(II) test (x=15%) of straight specimens. The period of the test was about 194 hours. Erosion losses were larger, considering the small test period, compared with those of AVT data under two-phase flow.

Figure 6 shows the experimental data for NT(II) of straight specimens. White square represents 500 hours data and black square represents 3500 hours data. As the test period increased, erosion losses became larger.
Figure 7 shows the experimental data for NT(III) (x=15%) of inner and outer bend specimens.

White symbol represents 500 hours data and black symbol represents 3500 hours data. As the test period increased, erosion losses of outer bend specimens became larger.

Figure 8 shows erosion loss of NT(Ⅱ) (straight specimens) as a function of test period. Erosion loss increases as the test period increases. Values of erosion loss in the figure are the mean ones. For 194 hours test, mass flow rate was rather larger than those of 500, 1000, 1500 and 3500 hours tests.

Figure 9 shows the operation data of the CTL for NT (Ⅱ) and NT (Ⅲ) tests of 1000 hours. Abscissa represents operation period and ordinate represents operational temperature, pressure, water flow rate and steam flow rate.
During the test, 2 times stops of operations were caused by loop troubles.

3.3 AVT Erosion Results under Single-Phase Flow

AVT erosion experiments under single-phase flow consist of AVT(V) (heated water, straight specimens) and AVT (VI) (steam, straight and bend specimens) ones.

In Table 3 are listed the experimental data for AVT (V) of straight specimens. The test period is 691 hours. Erosion losses of 23 m/s water velocity were much larger than those of 6 m/s, and erosion losses under heated water flow were much larger than those under two-phase flow and those under steam flow.

Figure 10 shows the experimental data for AVT (VI) (45

m/s steam velocity) of straight specimens and bend specimens. Erosion losses under steam flow were very small in general even with high steam velocity (45 m/s).

3.4 Analyses of Specimen Surface

By the use of SEM, observations were performed on the specimen inner surfaces after the tests. Oxide films cover all the surface of the specimen, and in several places oxide films are observed to be peeled off by erosion. However, the degrees of erosion attacks are not so severe because the depths of the peeled-off places are shallow.

Depth profiles of oxide films were analyzed by the use of AES with etching successive layers of film by argon-gas ion bombardment. Figure 11 shows the AES spectrum of NT(Ⅲ) specimen surface, for instance. Abscissa means etching time which corresponds to depth from the film surface and ordinate means weight percentages of elements. In general, the thickness of oxide film for NT tests was larger than those of AVT tests.

Moreover, X-ray diffraction analyses were performed on the erosion specimens to determine the chemical formulae of oxide films. By the analyses, the oxide films were determined to be mainly consisted of the following oxides.

$$\alpha Fe_2O_3, \quad FeO, \quad Fe_3O_4$$

After the erosion tests, oxide films of specimen surface were removed by reagents in order to obtain the specimen weight W_1 of equation (1). At the time, the weight dif-

ferences were obtained betwee before and after the film removals. These data with AES analyses yielded the density of oxide films. The thickness of oxide films and the density of oxide films were dependent on the environment such as water chemistry and test periods.

4. Discussion

4.1 Discussion on Erosion Data

As shown in Table 3 erosion losses of type 316L stainless steel were not so increased according as the increase of two-phase flow velocity. This phenomenon was partly due to our experimental procedure that steam-phase velocities were changed by changing specimen diameter. If one uses only one diameter specimen and increases the total mass flow rate, erosion losses of specimens will increase gradually. Erosion losses of NT(I) test and NT(II) (194 hours) test were larger than those of NT (II) (500, 1000, 1500 and 3500 hours) test, which can be interpreted by the difference of total mass flow rate. We proposed the quantitative erosion equation (8) in 5.1, which includes this physical meaning in it.

On the other hand, under single-phase flow like heated water as shown in Table 3 erosion losses of materials were direcly dependent on the flow velocity, that is, erosion losses were increased drastically according as the increase of the flow velocity.

As shown in Figure 8 and Table 3, the rate of erosion loss (the slope in Figure 8) were rather larger at the shorter test period and became smaller as the test period became longer.

Under two-phase flow, erosion losses for NT tests were obtained in the present data to be 2 ~ 3 times larger than those for AVT tests, which was mainly ascribed to the water chemistry. Differences of erosion losses between straight

specimens and bend specimens (350mmR) were not so large and almost the same order under two-phase flow conditions. Contrarily, under single-phase flow conditions, these differences have been reported to be large in some papers.

Comparisons are made here using the present data on erosion losses among under heated water, under two-phase water-vapour (x=10 ~ 60%) and under steam. Erosion losses were the largest under heated water flow and were the smallest under steam flow. Erosion losses under two-phase water-vapour flow were in the middle of them and erosion losses did not differ so largely in the range of steam quality 10 ~ 60%.

From the standpoint of the design for ATR Demonstration Plant, it is concluded that the reduced thickness of the outlet pipe by erosion loss during the reactor life is much smaller than that of the surplus thickness of the outlet pipe [4].

4.2 Porosities of Oxide Films

Porosities of oxide films are affected by the fluid environment such as water chemistry, flow velocity, flow pattern, test period and temperature. By the results of AES data, film thickness, density of film and chemical formulae of oxide, porosities in the film are to be estimated [4]. For instance, porosities at molecule level for AVT(II) test and NT(I) test were estimated to be 12% (film thickness $\simeq 1\mu m$) and 26% (film thickness $\simeq 3\mu m$), respectively. Porosities for NT tests were in general larger than those for AVT tests.

Under NT conditions, erosion-corrosion is considered to be more increased than that under AVT conditions. Porosities are determined by the fluid environment and test period, we think.

5. Propositions of Semi-Theoretical Erosion-Corrosion Equations

5.1 Erosion-Corrosion Equations under Two-Phase Flow

Under water-vapour two-phase flow (steam quality 0.1~0.7) at about 280°C and 70 kg/cm^2, erosion-corrosion losses for NT and AVT tests were obtained to be almost constant for steam phase velocities 10~60 m/s, of which data are shown in Table 3 and figures above.

This constancy is attributed to our experimental procedures such that we performed erosion experiments using 73.7, 62.1, 49.4 and 38.3 mm inner diameter specimens with constant flow rate, we think. For the two-phase erosion study, it is very important to consider the flow pattern and its dynamics. The flow pattern of the two-phase flow in this work are classified into annular mist flow type [2].

Figure 12 shows the schematic of annular two-phase flow [5]. The large-disturbance liquid waves (LD waves) proceed smoothly on sublayer flows. Entrainments are produced near the top of the LD waves by the attack of acceralated steam flow. The speed of LD waves is one order higher than that of sublayer [5], so that the attack of LD waves on pipe surfaces is weak, we think.

In 1985, M. Koike [4] already proposed the following erosion equation by his model that the erosion loss of straight pipe under two-phase flow is contributed mainly by sublayer momentum flux (kg·m^2/m·sec^2), not by LD waves.

$$E_T \sim \frac{\rho_L Q_S^2}{2\pi r \ell A_S} \simeq \frac{W^2 V_G^0 \{F(x, V_G^0)\}^2}{4\pi^2 \ell \rho_L r^3} \quad , (2)$$

by introducing

$$Q_S \rho_L = WF(x, V_G^0) \quad , (3)$$

$$G_S / G_0 = F(x, V_G^0) \quad , (4)$$

where E , ρ_L , Qs, r, ℓ and As are erosion loss, liquid phase density, sublayer volume flow rate (m^3/s), pipe radius, flow length and the cross section area of sublayer flow, respectively. W, V_G^0 , F(x, V_G^0), Gs and Go are total mass flow rate (kg/s), superficial steam velocity, mass flux ratio which is a function of steam quality and superficial steam velocity, mass flux ($kg/m^2.s$) of sublayer flow and total mass flux of two-phase flow.

The sublayer volume flow rate, Qs (AsVs) are not known at about 280°C except those at room temperature [5], so that the extensions of this value to 280°C were performed [4] by the function F which represents the two-phase flow pattern. Actually there are direct correlation in the flow pattern of two-phase flow between steam quality and mass flux by Yanai [6] and between the superficial steam velocity, V_G^0 , of two-phase flow and mass flux by Sekoguchi [5].

Using the two-phase flow dynamics experimental data at room temperature [5], we obtained the values of F as functions of steam quality and superficial steam velocity by re-arranging and re-calculating the data of annular two-phase flow dynamics. Using the re-arranged and re-calculated data about F, we approximately made equation F as

$$F(x, V_G^0) = -2.7\times10^{-6}(V_G^0 - f(x))^3 + 4.7\times10^{-4}(V_G^0 - f(x))^2 - 0.024(V_G^0 - f(x)) + 0.434 \quad , (5)$$

$$f(x) = -65.6(x-0.26)^3 - 1.56(x-0.26)^2 + 27.9(x-0.26) \quad , (6)$$

within the range of

$$\begin{cases} V_G^0 = 10\sim60 \text{ m/s} \\ x = 0.1\sim0.7 \end{cases} \quad , (7)$$

where x is steam quality

As shown in Figure 9, erosion loss is rather rapid at the time 0~500 hours and becomes slower at the time 1000~3500 hours. By mainly using 1000~3500 hours data with slight consideration of 0~500 hours data, we made the quantitative two-phase flow erosion equation for 316L stainless steel on the basis of equation (2) and (5).

We obtained the following equation as

$$E_T = 0.058\, K_1 K_2 \frac{F^2 W^2 V_G^0}{4\pi^2 \rho_L r^3} \quad , (8)$$

$$K_1 = \begin{cases} 1 & \text{for AVT} \\ 2\sim3 & \text{for NT(}\sim\text{300ppb DO)} \end{cases} \quad , (9)$$

$$K_2 = \begin{cases} 1 & \text{for straight pipe} \\ 1\sim2 & \text{for bend pipe (350mmR)} \end{cases} \quad , (10)$$

where E_T is erosion loss in the unit of μm/year and unit of W, V_G^0 , ρ_L and r is MKS one. This equation is to be used within the range of equation (7). The agreement between experimental data and calculated one by equation (8) is rather good.

Experimental results of erosion loss of bend specimens (350 mmR) were almost the same order as those of straight specimens in the present work. So that K_2=1~2 is recommended here. Under two-hase flow, the quantitative erosion-corro-

sion equation (8) with (5) and (6) was proposed here as a semi-theoretial equation.

5.2 Erosion-Corrosion Equations under Single-Phase Flow

For the erosion-corrosion under single-phase flow, AVT (V) data of high-temperature high-pressure water (about 280°C, 70kg/cm^2) and AVT(VI) data of high-temperature high-pressure steam (about 280°C, 70kg/cm^2) were obtained in the present work as shown in Table 3. By the use of the data, we have made the erosion-corrosion quantitative equation for single-phase flow.

As shown in Table 3 erosion-corrosion losses were drastically affected by the flow velocity of heated water even under AVT conditions. Firstly, from the standpoint of mechanics of fluid flow, erosion-corrosion under single-phase flow is considered. In the present case, Reynolds numbers, $Re=Vd/\nu$ (V: Velocity, d: pipe diameter, ν : kinematic viscosity) were estimated as $Re=3.5\times10^6$ & 6.7×10^6 for AVT(V) test and $R3=3.3\times10^6$ for AVT(VI) test. These flow patterns are all classfied into turbulent flow which consists of laminar sublayer, buffer layer and turbulent region [7]. As the laminar sublayer and buffer layer are very thin thickness flow and very close to pipe wall, we think like two-phase flow model that the momentum flux of these flows dominantly affect erosion-corrosion loss of pipe. Like the simular method as that performed for the two-phase flow with the consideration of our experimental data, we have origi-

nally made the following equation for erosion-corrosion under single-phase flow as

$$E_s = 34 K_1 K_2 K_3 \rho (\delta_s \bar{v}_s^2 + \delta_b \bar{v}_b^2) \quad , (11)$$

$$\begin{cases} \delta_s = 5\nu/\sqrt{\tau_w/\rho}\ , \ \delta_b = 25\nu/\sqrt{\tau_w/\rho} \\ \bar{v}_s = 2.5\sqrt{\tau_w/\rho},\ \bar{v}_b = \sqrt{\tau_w/\rho}\left(5 + 5\ell n \frac{17.5}{5}\right) \\ \tau_w/\rho = \lambda V^2/8,\ \lambda = f(Re,\ k/r) \end{cases} \quad , (12)$$

$$K_1 = \begin{cases} 1 & \text{for AVT} \\ 2 \sim 3 & \text{for NT } (\sim 300\text{ppb}) \end{cases} \quad , (13)$$

$$K_2 = \begin{cases} 1 & \text{for straight pipe} \\ \text{EPRI data} & \text{for bend or tee [9]} \end{cases} \quad , (14)$$

$$K_3 \begin{cases} 1 & \text{for water} \\ 1/3 & \text{for steam} \end{cases} \quad , (15)$$

where Es is erosion-corrosion loss in the unit of μm/year for 316L stainless steel under single-phase flow. δ_s , δ_b , $\bar{v}_s$ and $\bar{v}_b$ are laminar thickness (m), buffer layer thickness (m), mean velocity of laminar sublayer (m/s), and mean velocity of buffer layer (m/s), respectively. ν , τ_w and ρ are kinematic viscosity (m^2/s), shear stress on pipe, and liquid or steam density (kg/m^3). λ and V are frictional coefficient of pipe, and single-phase flow velocity (m/s), respectively. λ is expressed with the parameter Re and k/r (k is pipe surface roughness) by Moody [8].

Our data of AVT(V) and AVT(VI) were in good agreement with values calculated by equation (11). For steam, K_3 =1/3 should be used if considering our experimental results. K_2 value for bend pipe or tee pipe are unknown although FPRI

data [9] are to be used. K_1 value for NT test is unknown but 2 ~ 3 is recommended here.

For single-phase flow, the erosion-corrosion quantitative equation (11) was proposed here, considering flow mechanism and experimental results.

5.3 The Erosion/Corrosion Equation for all Metals and Alloys in the World

For two-phase flow, the quantitative erosion-corrosion equation (8) was proposed here as a semi-theoretical equation. Also, for single-phase flow, the quantitative erosion-corrosion equation (11) was proposed. However, the meaning of coefficients 0.058 K_1 for two-phase flow and $34K_1$ for single-phase flow are not described yet. These coefficients are attributed to material properties and to flow environments such as water chemistry, which were already proposed by M. Koike [4], although not quantitatively described.

Here, we have originally created semi-theoretically the following equation for all metals and alloys as

$$(\Delta g^{*}_{M\to i} - \Delta g_{M\to i})\,(\Delta\mu_{i\to o} - \Delta\mu^{*}_{i\to o})\,\sqrt{\frac{1}{B_{M-O}\,B_{M-M}}} \times \frac{P_{or}\,\delta^{-0.2}}{\sigma_y \cdot \rho_M} = \mathrm{Coef.} = \begin{cases} 0.058K_1 & \text{for two-phase flow} \\ 34K_1 & \text{for single-phase flow} \end{cases} \quad , (16)$$

where $\Delta g_{M\to i}$, $\Delta\mu_{i\to o}$, $\Delta g^{*}_{M\to i}$ and $\Delta\mu^{*}_{i\to o}$ are the free energy change per gram equivalent of the reaction that $M \to M^{n+} + ne^{-}$ [10], the chemical potential change of the reaction that

$M^{n+} + \frac{n}{2} H_2O \rightarrow MO_{\frac{n}{2}} + n^{H+}$ (11), the free energy change per gram equivalent for the ideal metal and the chemical potential change for the ideal metal of which values are defined by us, respectively. B_{M-O}, B_{M-M}, P_{or}, δ, σ_y and ρ_M are bond strength between metal and oxygen, bond strength between metal and metal (12), porosities of the corrosion film, thickness of corrsion film, yield stress of material and desity of material, respectively.

Porosities of corrosion film and thickness of corrosion film are affected by flow environments such as water chemistry, flow velocity, flow phase, flow pattern, temperature and test period (time), we think. In the present case for 316L stainless steel under two-phase flow, parameter difference in the equation (16) between AVT test and NT test is only in $P_{or} \cdot \delta^{-0.2}$ term. By the use of data already discussed, $P_{or} \cdot \delta^{-0.2} = 12(\%) \times 1^{-0.2}(\mu m) = 12$ for AVT and $P_{or} \cdot \delta^{-0.2} = 26(\%) \times 3^{-0.2}(\mu m) = 21$ for NT is to be calculated here. The factor $21/12 \simeq 2$ is already represented in K_1 in quation (9), of which values agree well each other.

As for another parameters also, the equation (16) is made so as to fit values of erosion/corrosion loss of all metals in general such as all pure metals, carbon steel, stainless steel, zirconium alloys and so on in the world. The detail explanation of this equation will be described in another paper.

6. Conclusions

(1) Erosion experiments of type 316L stainless steel under water-vapour two-phase flow (about 280°C, 70kg/cm^2) were performed by the use of Component Test Loop. Experimental results in Table 3 show that the erosion-corrosion losses were very small for not only straight pipe but also bend pipe. Erosion-corrosion losses for NT tests were 2~3 times larger than those for AVT tests.

(2) Using the present data for two-phase flow, with establishing semi-theoretical considerations, the quantitative erosion-corrosion equation (8) was originally made and proposed in the range of steam quality 0.1~0.7 and steam phase velocity 10~60 m/s.

(3) Erosion experiments of type 316L stainless steel under single-phase flow (heated water, steam) were also performed. Experimental results in Table 3 show that the erosion-corrosion losses were drastically increased with increasing flow velocities, even for AVT tests. Using these data with establishing semi-theoretical considerations, the quantitative erosion-corrosion equation (11) was originally made and proposed here. Besides, with the considerations of erosion/corrosion mechanism and with the present data as well as another data, the quantitative erosion/corrosion equation (16) was originally created and proposed for all metals generally in the world.

References

〔1〕 S. Sawai, "ATR and Its Specific Features', PNC Report, Japan, PNCT N341 84-17 (1984) November.

〔2〕 A.W. Bennet, G.F. Hewitt, H.A. Kearsey, R.K.F. Keeys, P.M.C. Lacey, AERE-R-4874 (1965).

〔3〕 S.G. Bankoff, "A Variable Density Single Fluid Model for Two-Phase Flow with Particular Reference to Steam-Water FLow", Trans. ASME, Ser. C. 82 (1960).

〔4〕 Mitsutaka Koike and T. Kitahara, Proceedings of 6th Annual Conference of Canadian Nuclear Society (1985) 8.1.

〔5〕 K. Sekoguchi, K. Nishikawa, M. Nakasatomi, H. Nishi and A. Kaneuji, Trans. JSME (in Japanese) 39 No.317 (1973)313.

〔6〕 M. Yanai, The Doctor Thesis of Kyoto University (1971).

〔7〕 see: Y. Kattoh, "Dennetsu Gairon", Yoh-Ken-Do Press (in Japanese) (1969).

〔8〕 D.F. Moody, Trans. ASME 66 (1944) 671.

〔9〕 EPRI report NP-3944, "Erosion/Corrosion in Nuclear Plant Steam Piping: Causes and Inspection Program Guidelines", (1985) April.

〔10〕 VL. CIHAL, "MEZIKRYSTALOVA KOROZE KOROZIVZDORNYCH OCELI", PRAHA, 1967, SNTLNakladatelsivi technícké literatury （和訳：日ソ通信社P.4）.

〔11〕 M. Pourbaix, Atlas of Electrochemical Equilibria in Aqueous Solutions, Pergamon Press (1966).

〔12〕 C.T. Lynch, Handbook of Materials Science, CRC Press (1974).

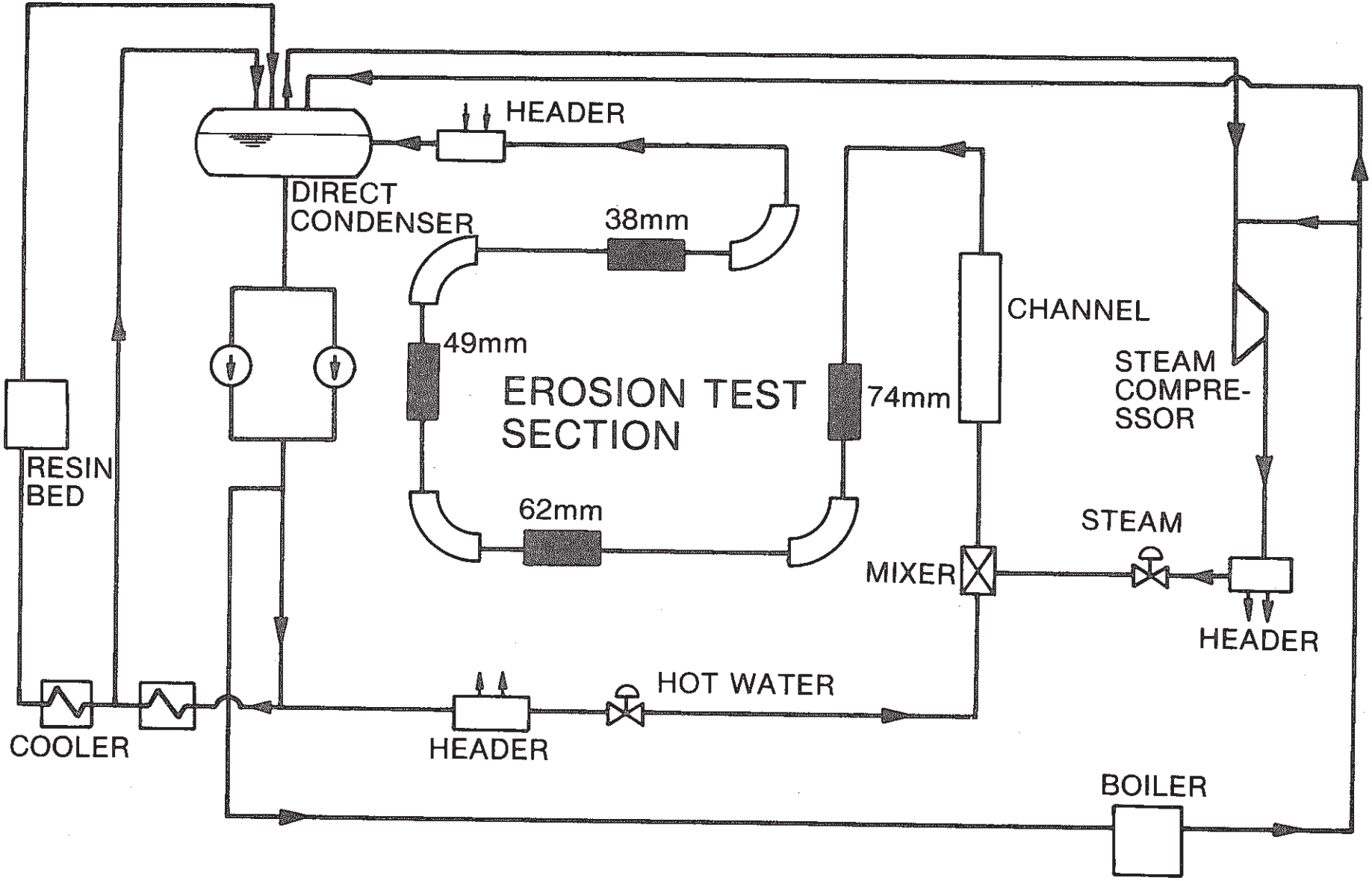

Figure 1 Flow Diagram of Component Test Loop.

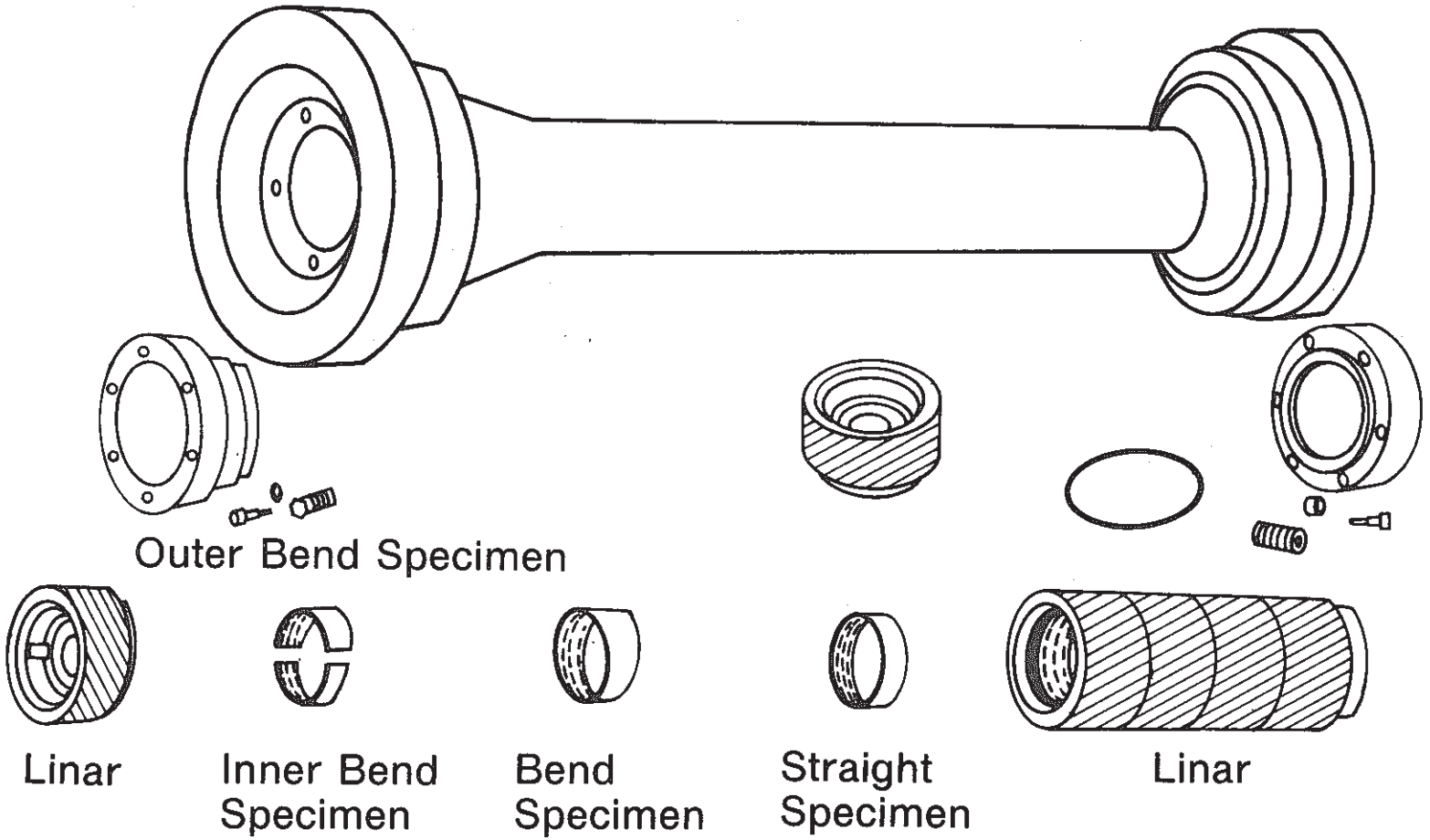

Figure 2 Erosion Test Apparatus

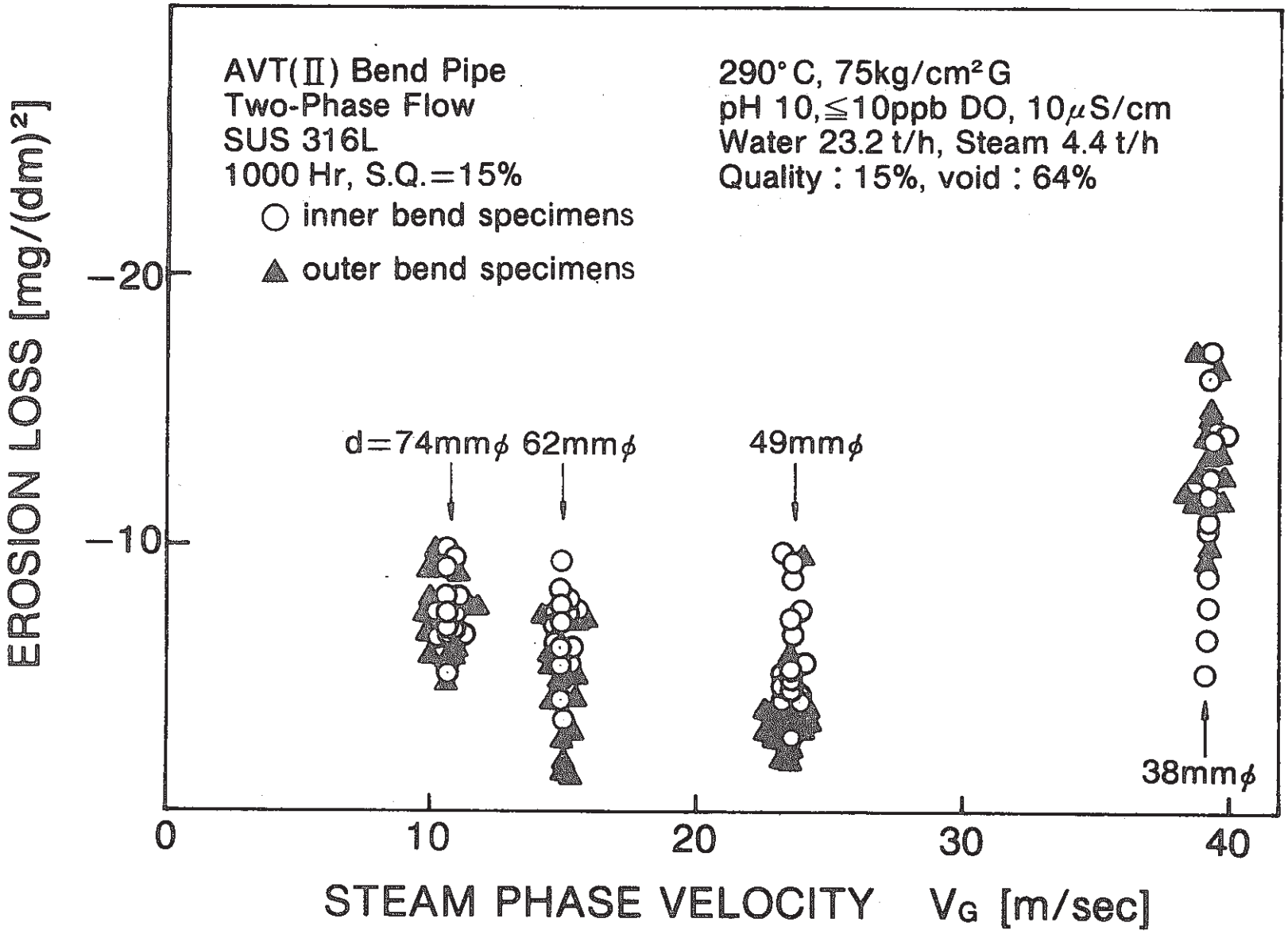

Figure 3 Experimental Results of Erosion Tests, AVt (Ⅱ)

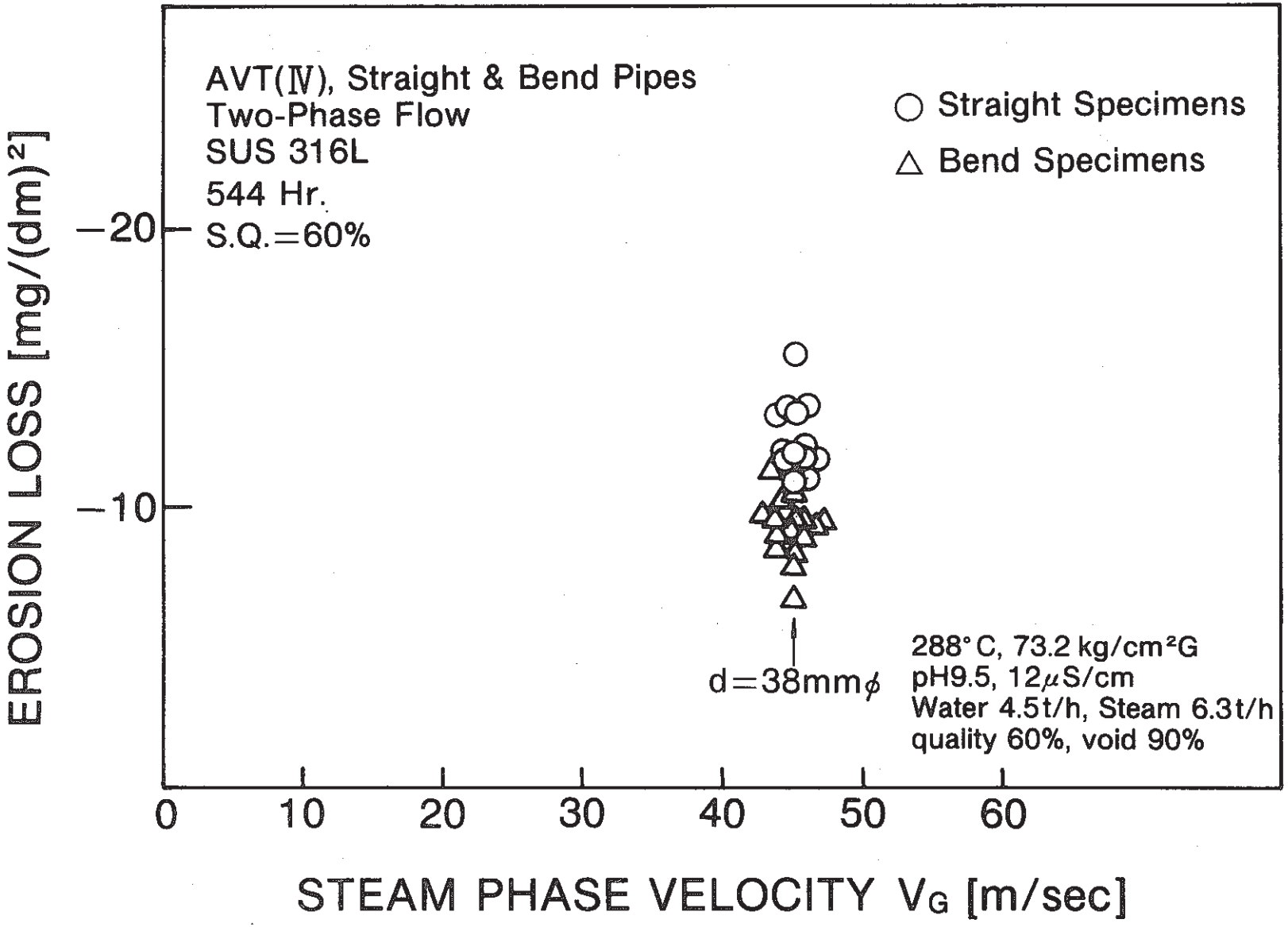

Figure 4 Experimental Results of Erosion Tests, AVT (IV)

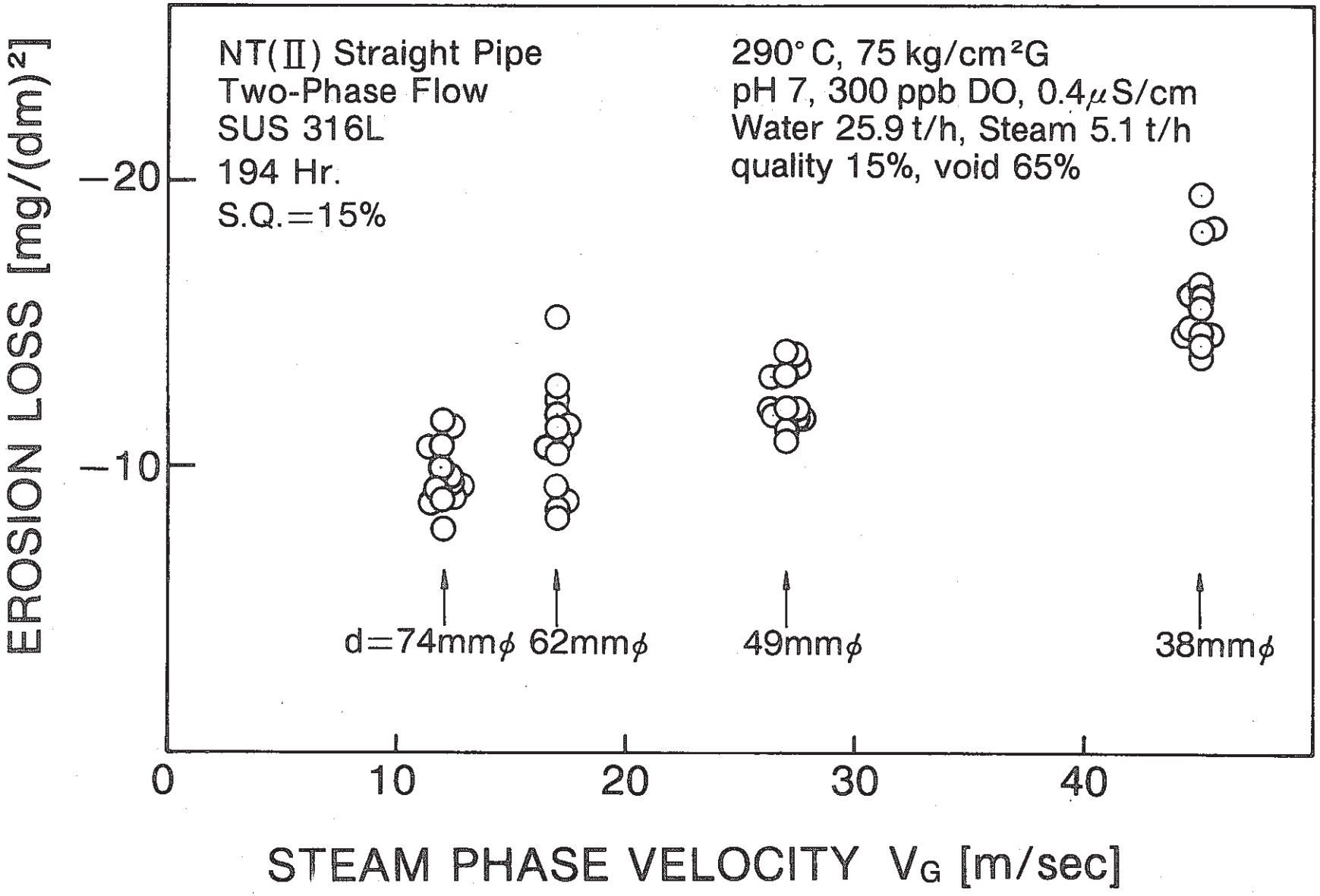

Figure 5 Experimental Results of Erosion Tests, NT(Ⅱ)

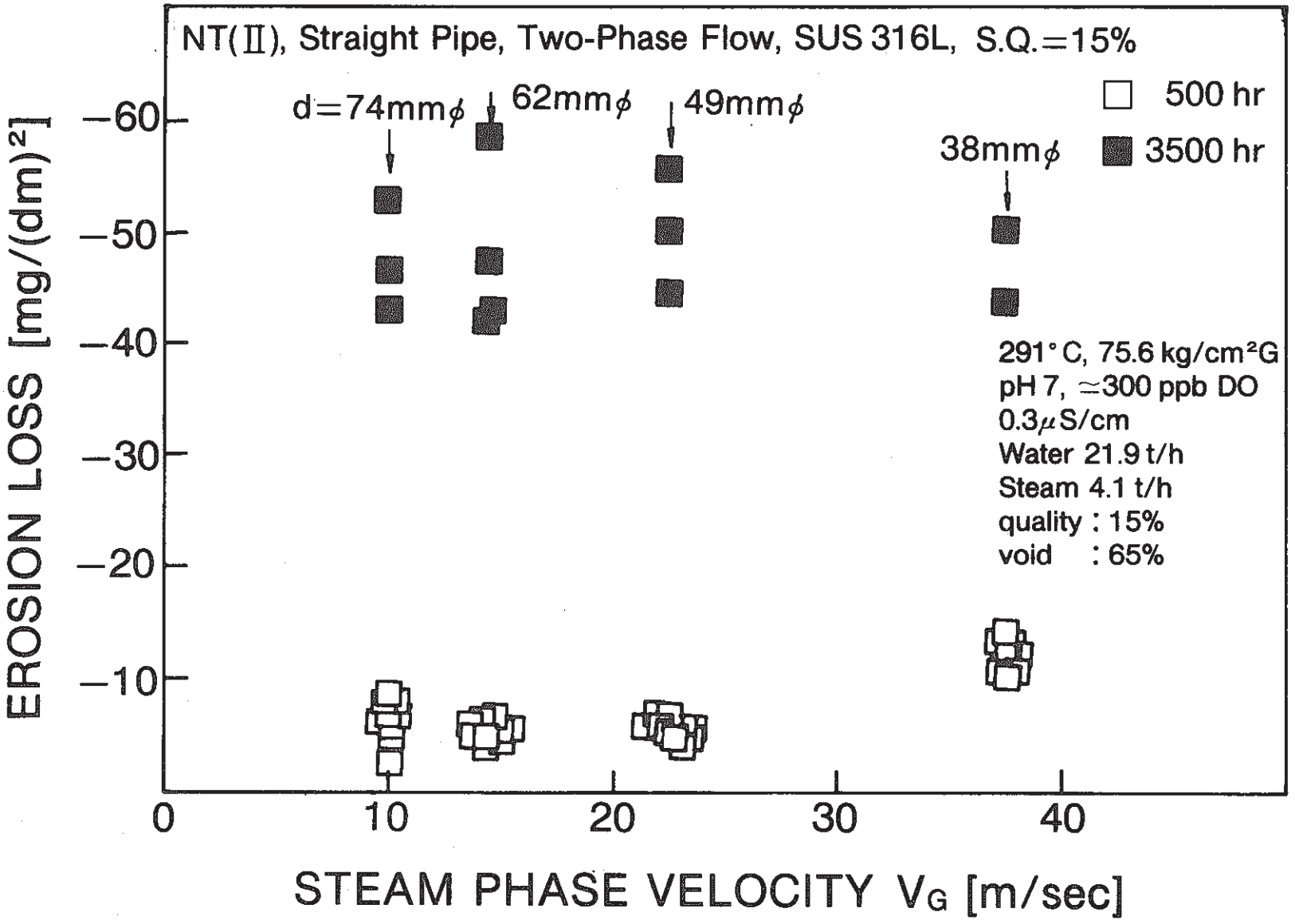

Figure 6 Experimental Results of Erosion Test, NT(Ⅱ)

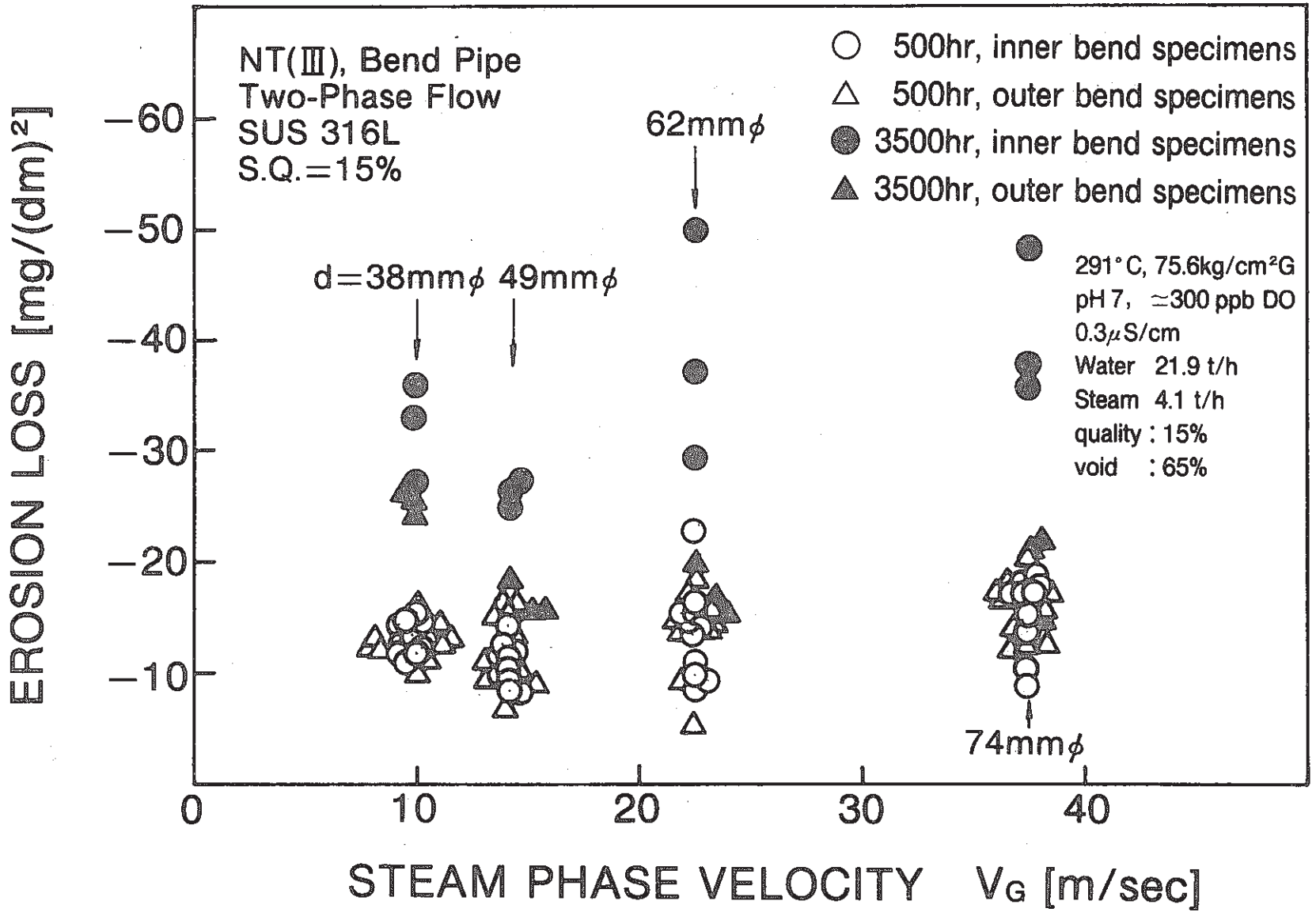

Figure 7 Experimental Results of Erosion Test, NT(Ⅲ)

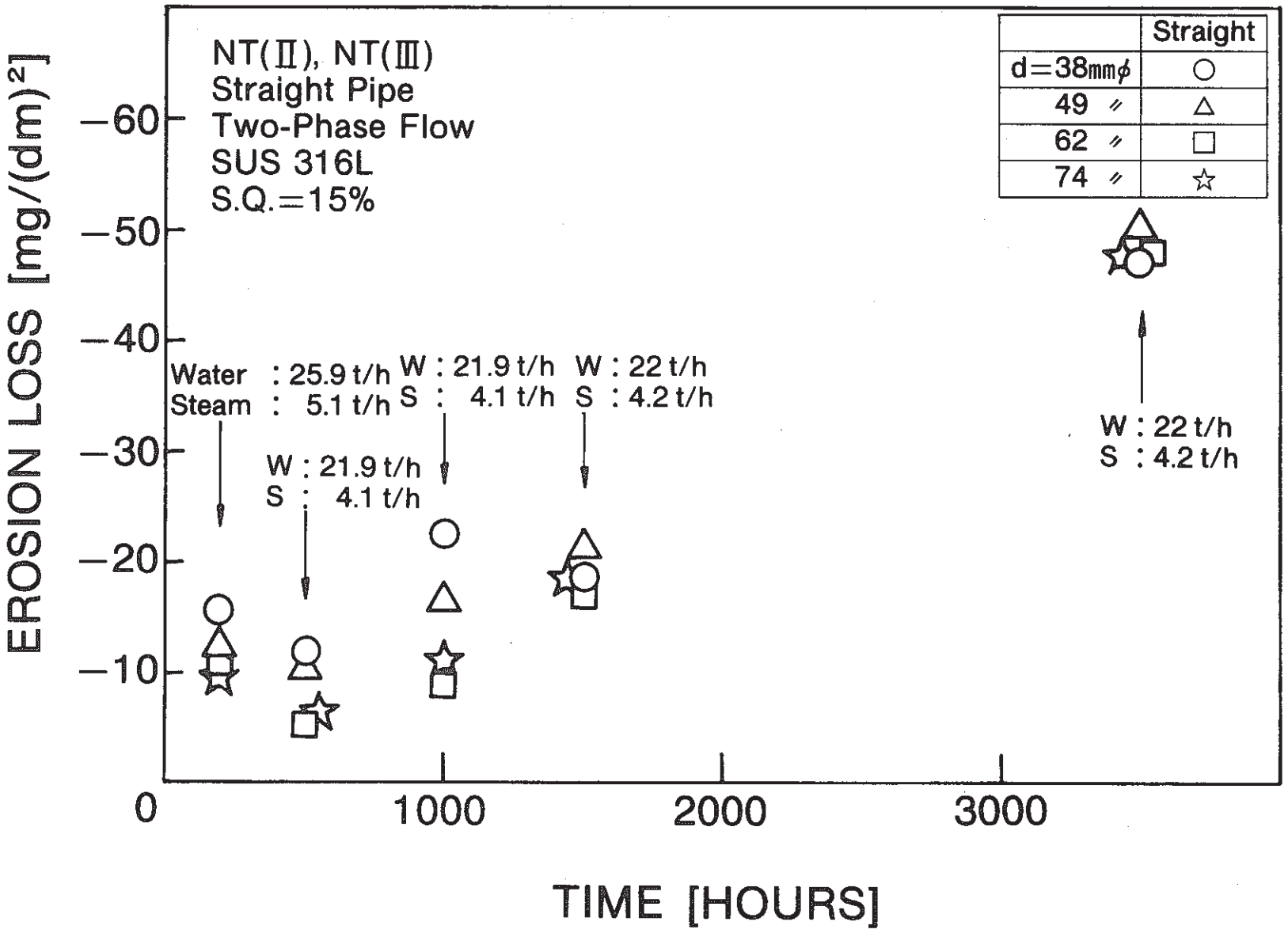

Figure 8 Relation between Erosion Loss and Time, NT(Ⅱ)

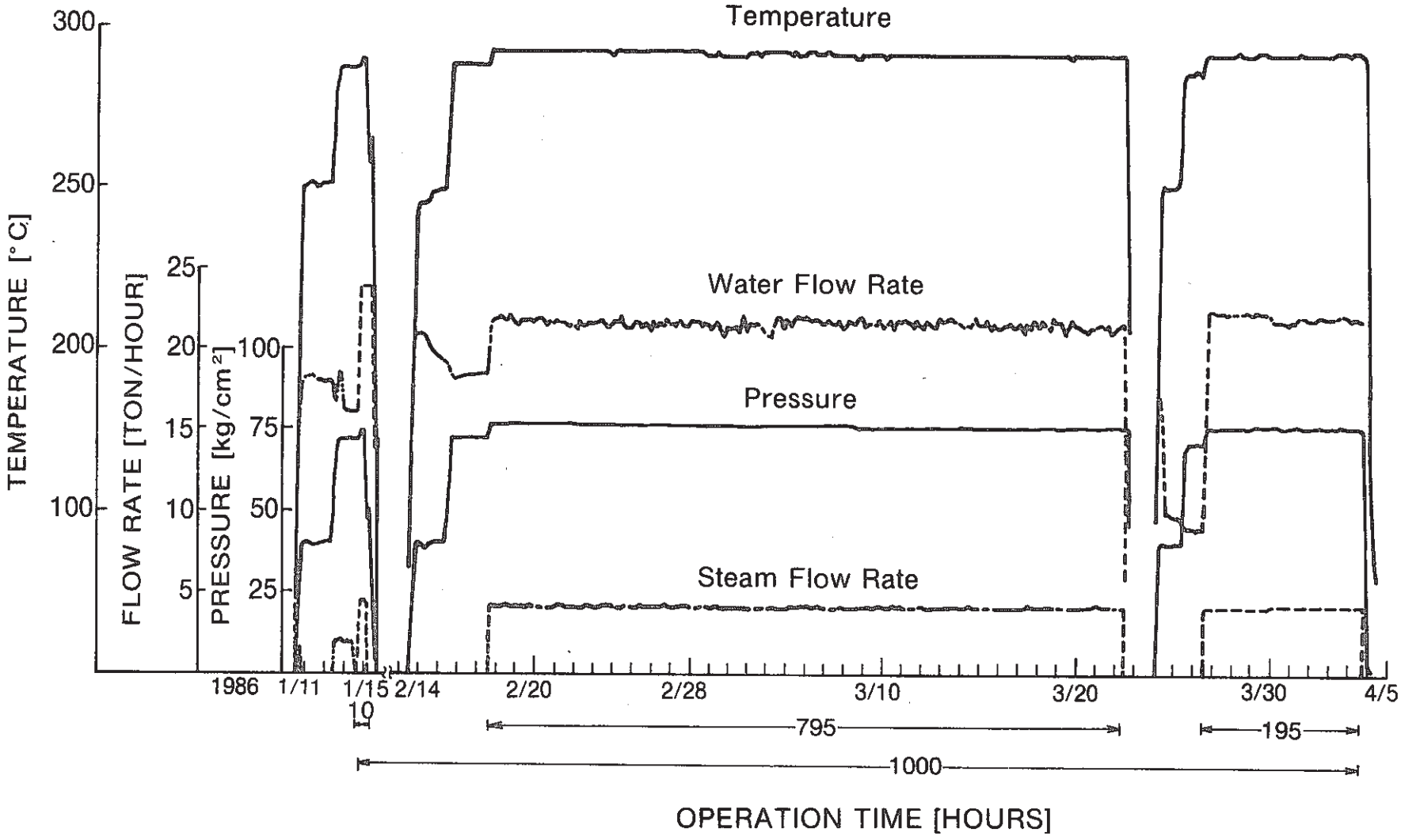

Figure 9 Operational Data of Component Test Loop for NT(Ⅱ) and NT(Ⅲ) Tests of 1000 hours

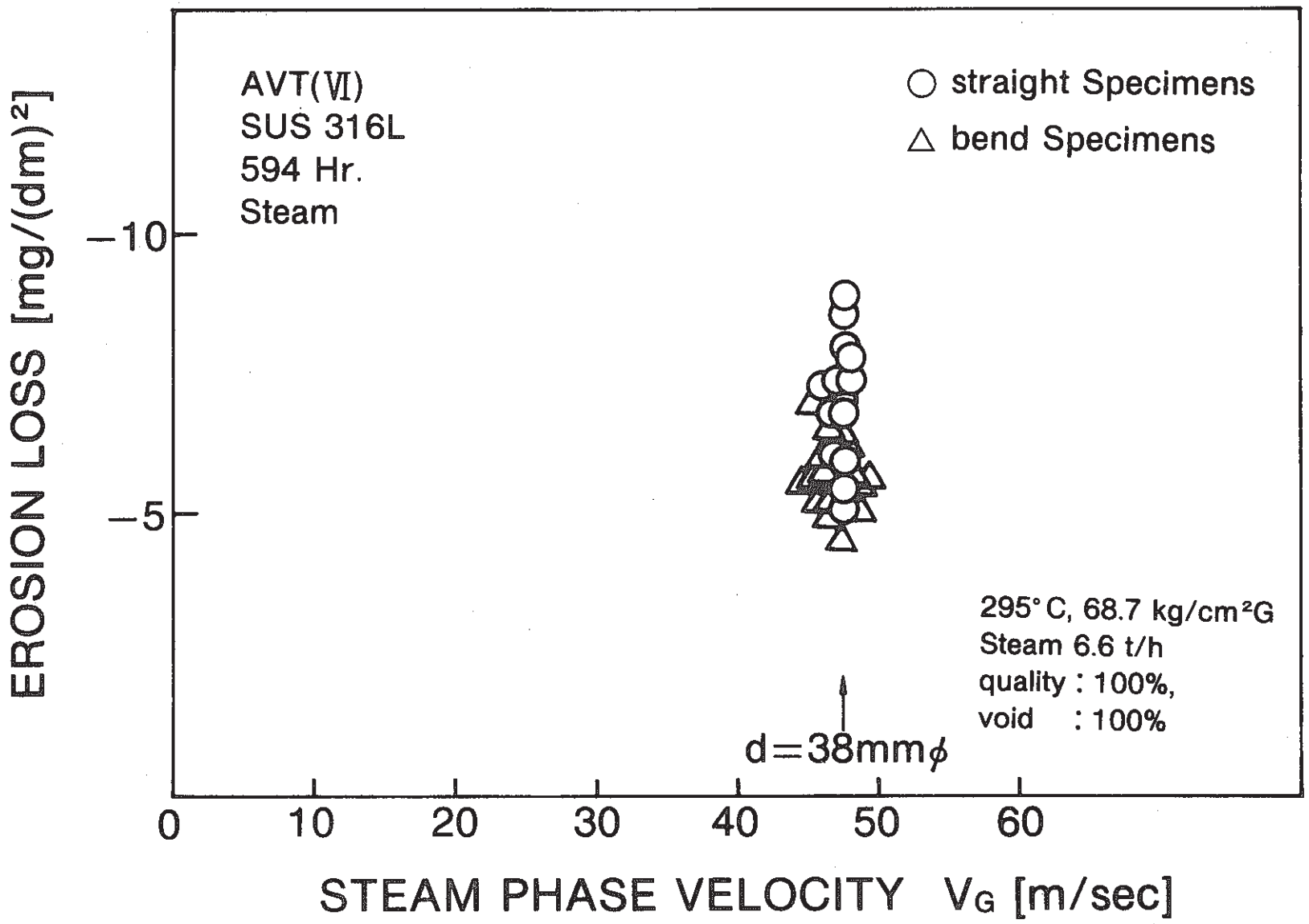

Figure 10 Experimental Results of Erosion Tests, AVT(VI)

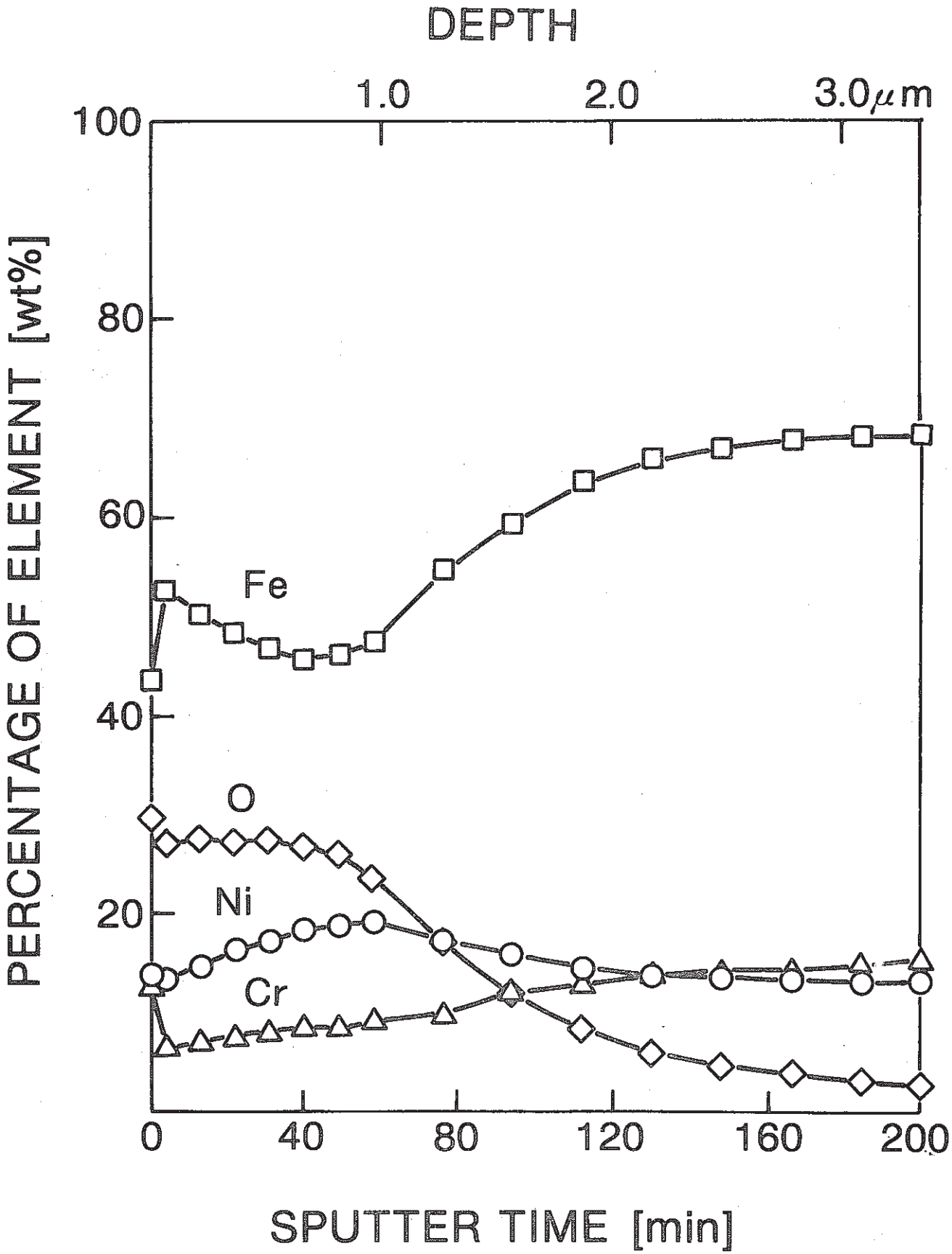

Figure 11 Depth Profile of Oxide Film Analysed by AES, NT(Ⅲ)

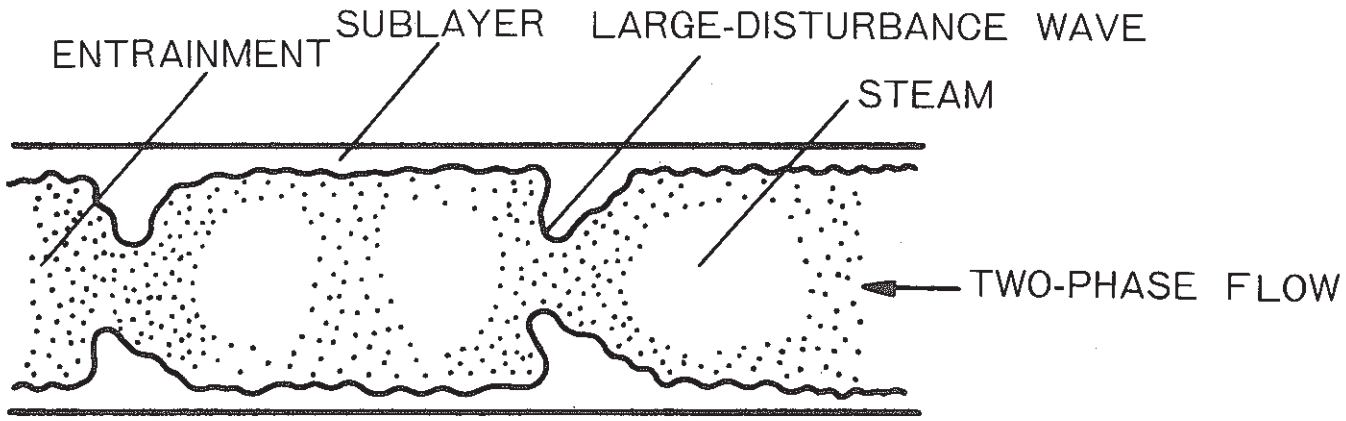

Figure 12 Schematic Diagram of Annular Two-Phase Flow

Table 1 CHEMICAL COMPOSITION OF TEST MATERIAL

	Fe	Cr	Ni	C	Mo	Mn	Si	P	S
SUS316L	67.14	16.67	12.13	0.024	2.04	1.48	0.48	0.031	0.009

Table 2 CONDITIONS OF EROSION TESTS

Two-Phase Flow (≃290°C, 75 kg/cm²)					
test	Steam quality (%)	Mass flow rate (t/h)	Test period (hr)	Water Chemistry	Steam Phase Velocity (m/s)
AVT(Ⅰ) (published)	15	W : 24.3* S : 5.16	S : 504, 1804** B : 504	PH : 10 CON : 10~15μS/cm DO : <2 ppb	11, 15, 24, 40
AVT(Ⅱ)	15	W : 23.2 S : 4.4	B : 1000		11, 15, 24, 39
AVT(Ⅲ) (published)	26	W : 18.9 S : 6.9	S : 898, 1158, 2057 B : 2057		14, 20, 32, 53
AVT(Ⅳ)	60	W : 4.5 S : 6.3	S : 544 B : 544		45
NT(Ⅰ) (published)	15	W : 24 S : 4.7	S : 170	PH : 7 CON : 0.4μS/cm DO : 120 ppb(NT(Ⅰ)) 300 ppb(NT(Ⅱ), NT(Ⅲ))	12, 17, 26, 44
NT(Ⅱ)	15	W : 25.9 S : 5.1	S : 194		12, 17, 27, 45
	15	W : 21.9 S : 4.1	S : 500, 1000, 1500 3500		10, 14, 23, 38
NT(Ⅲ)	15	W : 21.9 S : 4.1	B : 500, 1000, 1500 3500		10, 14, 23, 38
Single-Phase Flow					
test	Fluid	Mass flow rate (t/h)	Test period (hr)	Water Chemistry	Velocity (m/s)
AVT(Ⅴ)	Heated Water	W : 70	S : 691	PH : 9~10 CON : 5~10μS/cm	6, 23
AVT(Ⅵ)	Steam	S : 6.6	S : 594 B : 594		47

* W : Water, S : Steam

**S : Straight Pipe, B : Bend Pipe (350 mmR)

Table 3 EXPERIMENTAL RESULTS OF EROSION TESTS

(μm/year)

	Diameter (mm)			73.7	62.1	49.4	38.3
AVT(Ⅱ) steam quality =15% 1000 hr	V_G [m/sec] V_L [m/sec] V [m/sec]			11 6 6	15 8 9	24 13 14	39 22 23
	bend pipe		inner	0.8μ/y	0.7μ/y	0.7μ/y	1.3μ/y
			outer	0.8	0.5	0.4	1.4
AVT(Ⅳ) s.q.=60% 544 hr	V_G [m/sec] V_L [m/sec] V [m/sec]						45 14 24
	straight pipe						2.5
	bend pipe						1.9
NT(Ⅱ) s.q.=15% 194 hr	V_G [m/sec] V_L [m/sec] V [m/sec]			12 7 7	17 9 10	27 15 16	45 25 26
	straight pipe			5.5	6.1	7.0	8.9
NT(Ⅱ) s.q.=15%	V_G [m/sec] V_L [m/sec] V [m/sec]			10 6 6	14 8 8	23 12 13	38 21 22
	straight pipe		500hr	1.4	1.2	2.2	2.6
			1000hr	1.2	1.0	1.8	2.4
			1500hr	1.4	1.3	1.6	1.4
			3500hr	1.5	1.5	1.6	1.5
NT(Ⅲ) s.q.=15%	bend pipe	500hr	inner	2.9	2.3	3.0	3.4
			outer	2.8	2.7	3.0	3.5
		1000hr	inner	2.3	2.4	2.4	2.7
			outer	2.0	2.2	1.8	1.9
		1500hr	inner	1.4	1.3	2.0	1.9
			outer	1.1	0.6	0.7	0.6
		3500hr	inner	1.0	0.8	1.2	1.3
			outer	0.8	0.5	0.5	0.6
AVT(Ⅴ) heated water 691 hr	V_L [m/sec]			6			23
	straight pipe			2.9			7.5
AVT(Ⅵ) steam 594 hr	V_G [m/sec]						47
	straight pipe						1.3
	bend pipe						1.0